Multi-Angle Satellite Retrieval of Cumulus Thickness at the ARM TWP Site: Validation Tests

E. I. Kassianov, T. P. Ackerman, R. T. Marchand, and M. Ovtchinnikov
Pacific Northwest National Laboratory
Richland, Washington

Introduction

Most satellite-based analyses have been conducted using nadir-viewing sensors. The multi-angle Imaging SpectroRadiometer (MISR), recently launched on the (National Aeronautics and Space Administration (NASA) Terra platform, provides high-resolution measurements of reflectance at nine different viewing angles. We have suggested a new technique for retrieving cumulus vertical size (thickness) from multi-angle data and applied it to an early MISR dataset (Kassianov et al. 2000). The obtained results indicate that multi-angular MISR data have the potential for measuring cloud geometry. Two dependences form the basis of this technique: (1) for fixed horizontal cloud distribution, the probability of clear line of sight is a decreasing function of zenith viewing angle and (2) the rate of decrease of this probability depends on vertical cloud distribution. This paper presents validation analysis of this technique with both a model-data inverse problem and independent ground-based radar measurements. Collocated and coincident MISR data and ground-based observations at the Atmospheric Radiation Measurement (ARM) Tropical Western Pacific (TWP) site form the basis of this validation.

Multi-Angle Retrieval Technique

There are two basic steps of the retrieval of the average vertical size ΔH_{avr} of cumulus clouds (Kassianov et al. 2000). First, we estimate a set of the directional cloud fractions $N_{obs}(\theta) = \{N_{obs}(\theta_i), i = 1,\ldots,9\}$ from MISR observations (subscript "obs"). Second, we determine a threshold set $I_0(\theta) = \{I_0(\theta_i), i = 1,\ldots,9\}$ at which a difference $\Delta N_{obs} = N_{avr,obs} - N_{nadir,obs}$ peaks, where $N_{nadir,obs}$ is the nadir-view cloud fraction, and $N_{avr,\,obs} = \frac{1}{n}\sum_{i=1}^{n} N_{obs}(\theta_i)$, n = 9 is the average cloud fraction. Note, this difference characterizes the relative influence of the vertical variability of clouds on $N_{avr,obs}$. Finally, for a given horizontal distribution of cloud pixels, which is specified from nadir reflectance, model parameter (subscript "mod") $\Delta H_{avr,mod}$ is adjusted such that the equality $\Delta N_{mod} = \Delta N_{obs}$ is valid.

For a given horizontal distribution of cloud pixels, the directional cloud fraction $N(\theta)$ is a function of both the vertical size of cloud pixels, ΔH, and their base height base Z_{base}. The effect of ΔH variations on the directional cloud fraction $N(\theta)$ was illustrated (Kassianov et al. 2000). In particular, it was shown that $N(\theta)$ corresponding to the cloud field with variable ΔH can either be greater or less than $N(\theta)$, corresponding to the cloud field with constant ΔH (plane parallel geometry). The following simple example illustrates qualitatively the sensitivity of $N(\theta)$ to the cloud base variability. Let us consider a two-dimensional cloud (a cloud infinite in the y-direction) consisting of three pixels with the same horizontal and vertical size equal L (square-shaped pixels). Consider two cases. For case 1, all pixels have the same height of their bases: $Z_{base,i} = 0$, i = 1,2,3. For case 2, the first and the third pixels have the same base $Z_{base,1} = Z_{base,3} = 0$, while for the second (middle) pixel $Z_{base,2} = L$ (the second pixel is lifted up). For the case 1, the directional cloud fraction (cloud projection onto x-axis, or the size of the geometrical shadow) $N_1(\theta)$ is $L\times(3+\tan(\theta))$. For the case 2, the directional cloud fraction $N_2(\theta)$ is $L\times(3+\tan(\theta))$ if $\tan(\theta) <1$ and $2L\times(1+\tan(\theta))$ if $\tan(\theta) \geq 1$. Therefore, for the same horizontal and vertical pixel sizes, the inequality $N_2(\theta) \geq N_1(\theta)$ can be valid. For a cloud field, the dependence $N(\theta)$ on the cloud base variability will be more complex, because of the effects of screening of the incident radiation by surrounding clouds (mutual cloud shadowing). Since $N(\theta)$(off-nadir viewing angles) and ΔN can be sensitive to the cloud base variability, we will estimate the effect of Z_{base} fluctuations on the accuracy of ΔH_{avr} retrieval.

Model-Data Cloud Retrieval

To determine if multi-angle MISR data can be used to retrieve the average vertical cloud size ΔH_{avr} and to evaluate the accuracy of this retrieval, the *model*-data inverse experiments are performed. First, a three-dimensional (3D) broken field of marine clouds is simulated by using large-eddy simulation (LES) model. The obtained 3D cloud field is considered as a real 3D cloud field. Second, we simulate the MISR measurements by applying a Monte Carlo method. In the model inverse (retrieval) experiments, the simulated reflectance data are regarded as real observations. Third, we use these reflectances to retrieve average vertical cloud size, ΔH_{avr}, by applying the suggested technique of Kassianov et al. 2000. Finally, we compare the retrieved cloud product with the true value produced by the LES model. Since all properties of the simulated broken cloud field (available from LES simulation) are known exactly, the simulated measurements allow one to have precise control over the retrieval experiments.

Sounding data from the ARM TWP site are used to initialize and run the LES model. In particular, the latter is initialized using temperature and moisture profiles from the 23:31 Universal Time Coordinates (UTC) August 9, 2000, sounding at the Nauru, TWP site. Surface sensible and latent heat fluxes are computed applying an assumption of constant surface (ocean) temperature. Domain size for cloud field simulation is $10 \times 10 \times 2$ km^3 with 0.1-km horizontal and 0.033-km vertical resolution. Optical properties of simulated broken clouds are highly variable in both horizontal and vertical dimensions (Figure 1). The lifting condensation level (LCL) equals 0.72 km. The height of the cloud base above LCL, δZ_{base}, and cloud geometrical thickness, ΔH, varies over a large range (Figure 2). Their average values $\delta Z_{base,\ avr}$ and ΔH_{avr} are equal to 0.22 km and 0.20 km, respectively. The obtained 3D cloud field is considered as a real 3D cloud field.

For a given 3D cloud field from the LES model, we simulate MISR measurements at 672 nm by using a Monte Carlo method and periodical boundary conditions. For each pixel in the considered domain (total number of pixels is 10,000), reflectances are calculated at nadir and eight off-nadir viewing θ angles spread along the flight path: at 26.1°, 45.6°, 60°, and 70.5° in the forward direction (azimuth angle $\phi = 0$), and at 26.1°, 45.6°, 60°, and 70.5° in the aft direction (azimuth angle $\phi = 180$). The radiative

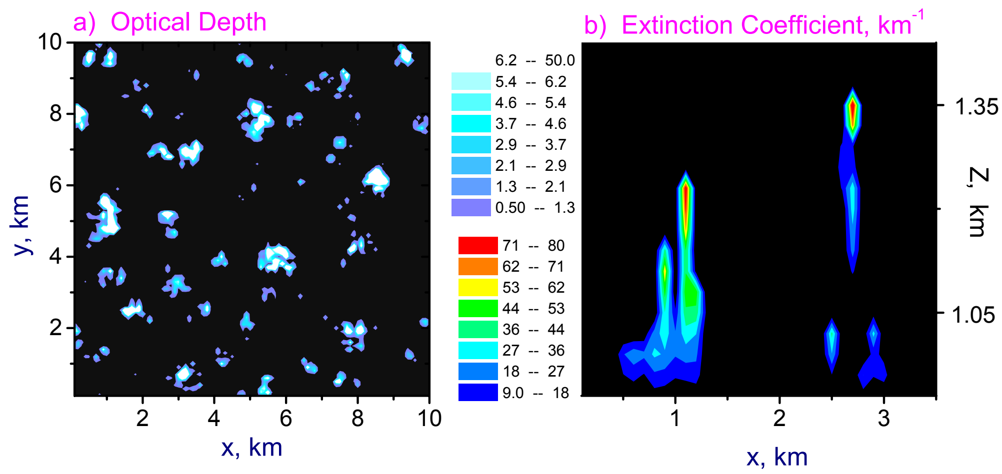

Figure 1. Cumulus clouds generated by LES model: a) horizontal distribution of optical depth, and b) an example of vertical distribution of extinction coefficient (a vertical cross section of the field of optical depth).

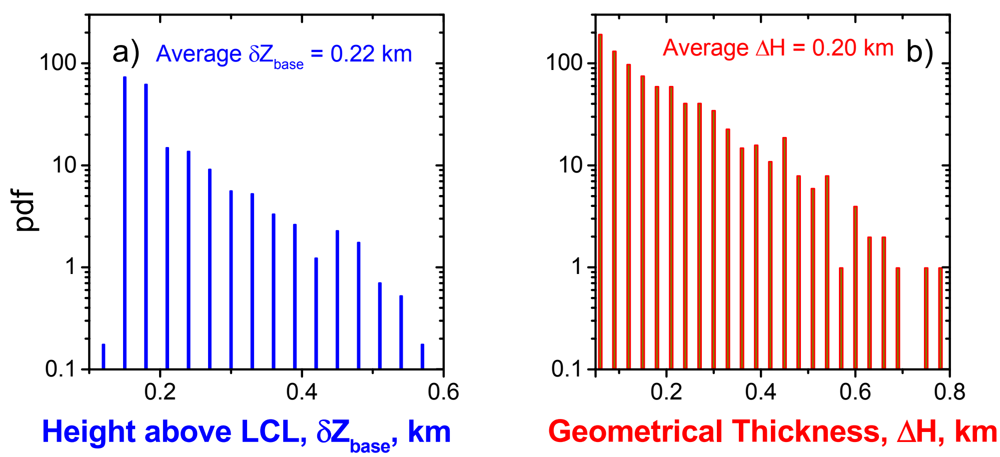

Figure 2. Cumulus clouds generated by LES model: probability density functions of a) height of cloud base above LCL, δZ_{base}, and b) cloud vertical geometrical size (thickness), ΔH.

calculations are performed for solar zenith and the azimuth angles equal 30° and 330°, respectively. Solar and viewing azimuth angles are measured from OY -axis. Note, this sun-sensor geometry is similar to the real one when MISR overpasses Nauru island at ~ 22:54 UTC. The Lambertian model with an albedo 0.06 is used for the ocean surface. Note, the Lambertian assumption is not appropriate for the ocean surface if a viewing angle is close to the forward scattering direction. However, for other viewing directions the Lambertian model can be considered as a reasonable approximation for the ocean surface (see e.g., Soulen et al. 2000). Because the scattering angle for given sun-sensor geometry is close to 180° (the forward scattering direction) for the viewing direction θ_6 ($\theta_6 = 26.1°, \phi = 180$), we do not include radiance $I(\theta_6)$ in our further analysis. In the model retrieval experiments, the simulated reflectance data are considered as observations.

Since the height of the base varies strongly (Figures 1, and 2), the question arises as to whether it is better to include δZ_{base} variability in ΔH_{avr} retrieval, or to assume a fixed value of δZ_{base}. With this aim in mind, two model-data experiments are performed. The only difference between these experiments is the assumption about the height of the pixel base above LCL, $\delta Z_{base,\ mod}$. In the first experiment, $\delta Z_{base,\ mod}$ is fixed and equals 0. In other words, all cloud pixels have the same cloud base at the LCL. In the second experiment, $\delta Z_{base,\ mod}$ is a random variable. For each cloud pixel the height of its base above LCL is chosen independently and equals $\delta Z_{base,\ avr} \times \alpha$, where α is a random variable uniformly distributed on (0,1) interval, $\delta Z_{base,\ avr} = Z_{base,\ avr} - \mathrm{LCL}$ (see Figure 2). Note, these two experiments do not take into account the correlation between $\delta Z_{base,\ mod}$ and Δh_{mod}.

Figure 3 gives results of these two experiments. The model curves $\Delta N_{mod,\ const}$ ($\delta Z_{base,\ mod}$ is constant) and $\Delta N_{mod,\ random}$ ($\delta Z_{base,\ mod}$ is random) are monotonically increasing functions of the average vertical cloud size $\Delta H_{avr,\ mod}$. In both experiments, the retrieved parameter ΔH is obtained with reasonable accuracy (about 0.1 km). However, the ΔH_{avr} retrieval is more accurate when the cloud base variability is included in the inversion process.

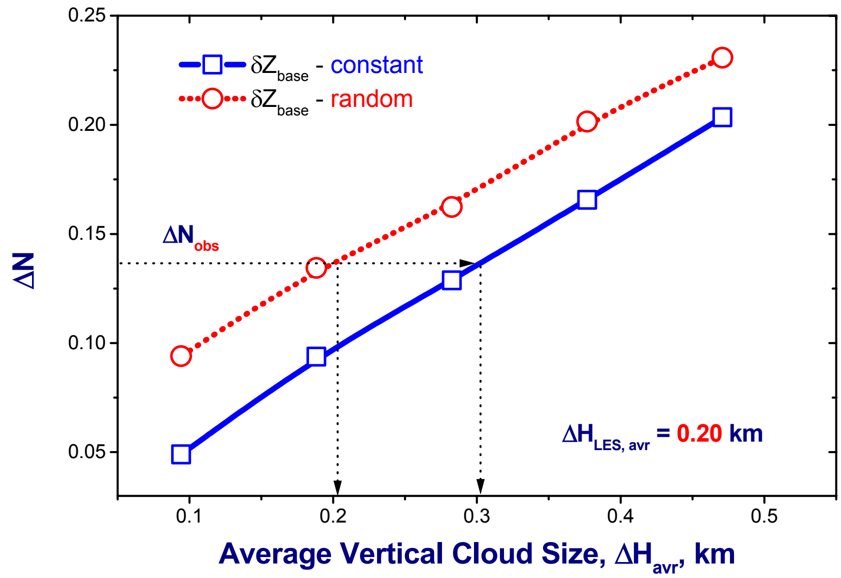

Figure 3. Difference ΔN_{mod} as a function of the average geometrical thickness ΔH_{avr} for two model-data experiments. The values of model parameters $\Delta H_{avr,\ const}$ and $\Delta H_{avr,\ random}$ such that $\Delta N_{mod,\ const}$ and $\Delta N_{mod,\ random}$ are equal to ΔN_{obs} are shown.

MISR-Data Cloud Retrieval

In addition to the model-data retrieval experiments, ΔH_{avr} retrieval is performed for a real MISR dataset. To validate the multi-angle retrieval technique, we use available satellite and radar ground-based measurements at the ARM TWP site (Nauru island). Note, the MISR passes Nauru once in nine days at ~ 22:54 UTC. Since the MISR has a 360-kilometer wide swath, a satellite image corresponds to a large area surrounding the island. In contrast, the temporal measurements from zenith pointing surface-radar represent line measurements (vertical cross section) along the wind direction. To review available satellite and radar measurements, the following two requirements are used. First, the satellite overpasses and ground-based measurements have been made at the same time during the day. Second, during the observations, the well-defined single layer of low cumulus clouds (without cirrus cloud contamination) has to occur over Nauru and in the area surrounding the island. Six available MISR overpasses of Nauru from March 2000 to December 2000 along with coincident ground-based measurements are examined. We found that data corresponding to the August 9, 2000, meet the two requirements. We used these data for our further analyses. Radar-derived cloud products are considered as reference.

The quantitative comparison between the satellte-retrieved cloud geometrical thickness with that determined from radar measurements will be meanful, if the cloud products are derived for the same cloud fields. In our analysis, the term "the same" means, that considered cloud fields have similar temporal (radar measurements) and spatial (satellite observations) bulk cloud statistics. In other words, we assume that these spatial and temporal statistics are interchangeable (ergodic approximation). The main bulk statistics, which describe single-layer broken clouds, are the cloud fraction N, and the mean (average) cloud horizontal, D, and vertical, ΔH_{avr}, sizes. Note, there is strong relationship between D and ΔH_{avr} (see, e.g., Benner and Curry 1998). We also assume that single-layer low broken cloud fields with similar N and D should have similar average vertical size ΔH_{avr}.

The bulk cloud statistics are functions of a sample size. The latter should be chosen from the balance of the following two opposite requirements. On the one hand, sample size should be small to avoid the problem of the cloud field temporal nonstationarity (spatial nonhomogeneity), but on the other hand, the sample size should be large to accurately represent the cloud field variability. Since the variability of a cloud field depends strongly on cloud type, sample size is a function of the cloud type as well. For example, for overcast stratocumulus clouds, good agreements between temporal and spatial statistics were obtained for the temporal resolution 0.5 hour (Dong et al. 1998), but for broken stratocumulus clouds, temporal and spatial statistics are in agreement for larger temporal resolution (about 1 hour) (Minnis et al. 1992). The broken cloud field over Nauru and surrounding area is highly variable (Figure 4), therefore we use a 1.5-hour temporal sample.

The radar data collected during this period (Figure 5) are applied to derive cloud statistics (Figure 6). We set radar sensitivity threshold equals to –50 dBz (see, e.g., Clothiaux et al. 1999). Note, the latter corresponds to the liquid water content of 0.01 g/m^3 (Fox and Illingworth 1997).

For a given sample size (1.5 hour) and threshold value (–50 dBz), we obtain the following *temporal* cloud statistics (subscript "t"): the cloud fraction, N_t, equals to 0.243; the average vertical geometrical size, $\Delta H_{t, avr}$, equals to 0.174 km; and the average cloud horizontal size (chord), $L_{t, avr}$, equals 177 sec. The height of the cloud base, Z_t, varies over a large range with the average value $Z_{t, avr}$ = 0.849 km and the minimum value $Z_{t, min}$ = 0.741 km (Figure 6). The latter is considered as LCL.

In practice, temporal size and statistics are often linked with spatial ones through the cloud-level wind speed. The latter is obtained from radiosonde measurements performed at 23:31 UTC with high vertical resolution (0.03 km). Since there is strong variability of the wind speed (from 7.3 m/sec to 10.1 m/sec) in the cloud layer (from 0.741 km to 1.281 km), we use the average cloud-level wind speed V_w.

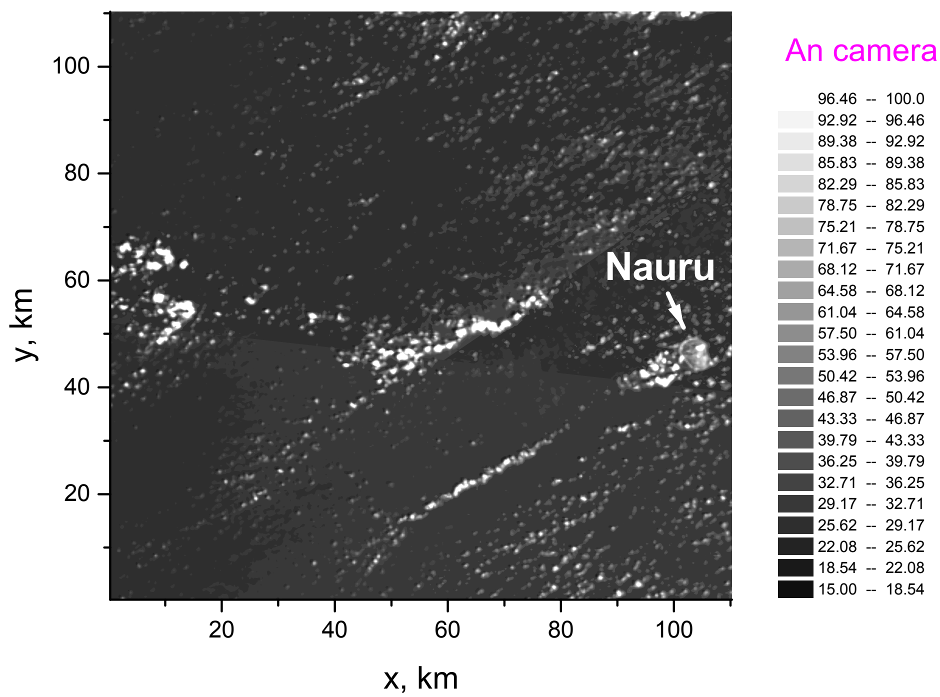

Figure 4. Cumulus clouds from MISR observations in 110 × 110 km^2 region surrounding and near ARM TWP site (Nauru), August 9, 2000: nadir reflectance (An camera).

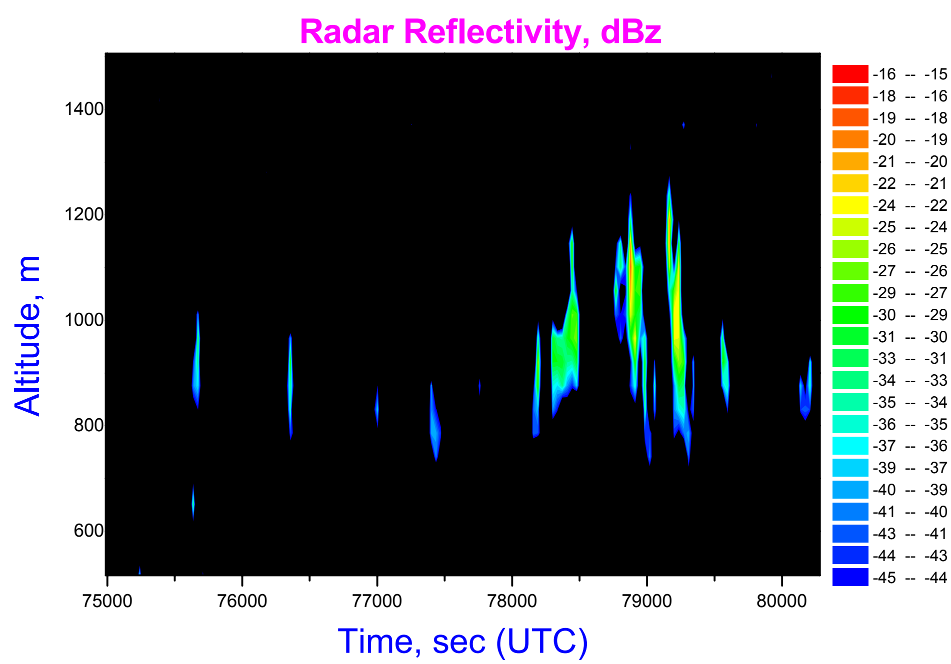

Figure 5. Cumulus clouds from ground-based radar measurements at ARM TWP site (Nauru), August 9, 2000: time-height cross section of radar reflectivity.

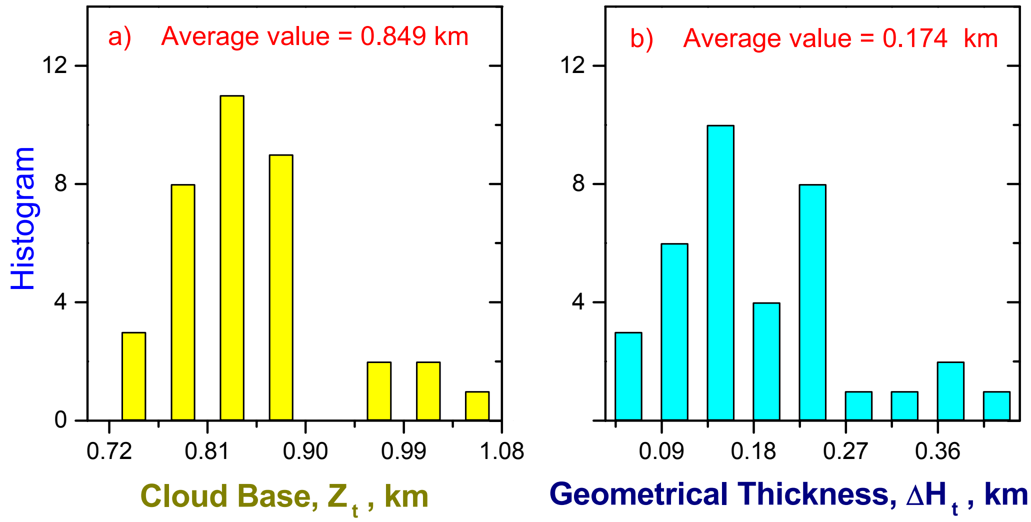

Figure 6. Cumulus clouds from ground-based radar measurements at ARM TWP site (Nauru), August 9, 2000: histograms of a) height of cloud base Z_t, and b) cloud vertical geometrical size (thickness), ΔH_t.

Assuming that this average value ($V_w \sim 8.5$ m/sec) is representative for the 1.5 hour temporal sample S_t, we estimate the corresponding spatial sample size, S_s, as $S_s = S_t \times V_w \sim 45$ km. In a similar way, the mean *spatial* cloud horizontal size (chord), L_s, is estimated as $L_s = L_t \times V_w \sim 1$ km.

From a large MISR image (110x110 km^2) we chose a smaller one (30x30 km^2) (Figure 7), which has bulk spatial statistics (cloud fraction and mean horizontal cloud chord) similar to those obtained from radar measurements. Satellite-derived variables for this MISR image have subscript “misr”. Following are the spatial statistics for the given MISR image the cloud fraction $N_{misr} = 0.252$, the mean cloud horizontal chords $L_{x,misr} = 1.21$ km (x-direction), $L_{y,\,misr} = 1.16$ km (y-direction). Note, that the cloud field, which corresponds to this MISR image, is about 70 km far away from Nauru Island (Figure 4). Then we apply the retrieval technique to derive the average cloud vertical size.

Similar to the model-data retrieval experiments considered in the previous section, two MISR-data retrieval experiments are carried out. In the first experiment, $Z_{base,\,mod}$ is fixed and equals $Z_{t,\,min}$ (considered as LCL). In the second experiment, $Z_{base,mod}$ is a random variable. For each cloud pixel, the height of its base above $Z_{t,\,min}$ is chosen independently and equals $\delta Z_{base,\,avr} \times \alpha$, where α is a random variable uniformly distributed on (0,1) interval, $\delta Z_{base,\,avr} = Z_{t,\,avr} - Z_{t,\,min}$ (see Figure 6). Results of these two experiments are presented in Figure 8. In both experiments, the retrieved parameter ΔH_{avr} coincides closely with the surface-based value $\Delta H_{t,\,avr}$ closely: the maximum difference between ΔH_{avr} and $\Delta H_{t,\,avr}$ is about 25%. Including the cloud base variability in the ΔH_{avr} retrieval allows one to decrease this difference.

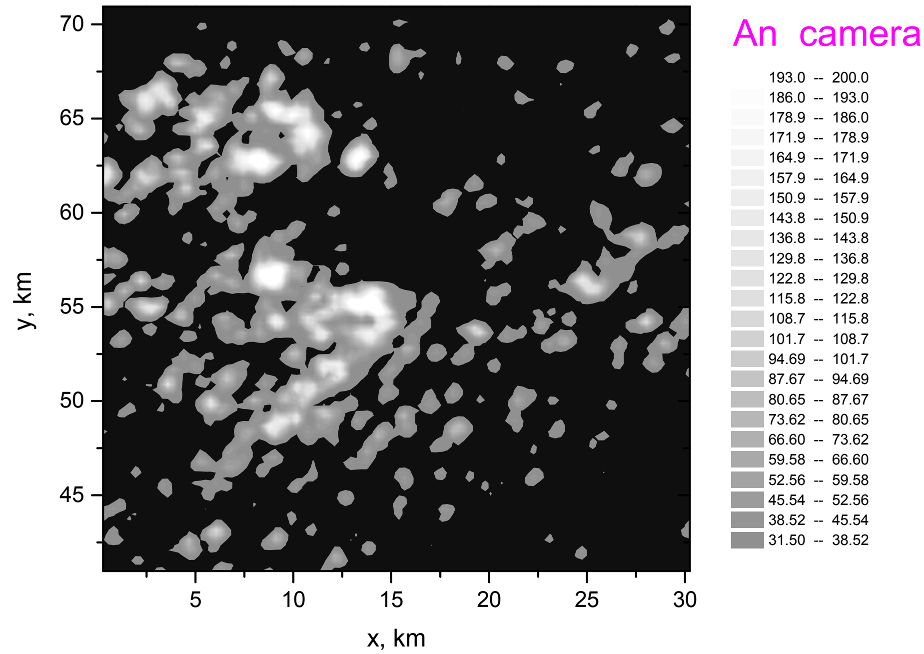

Figure 7. Cumulus clouds from MISR observations in 30 × 30-km^2 region near the ARM TWP site (Nauru), August 9, 2000: nadir reflectance (An camera).

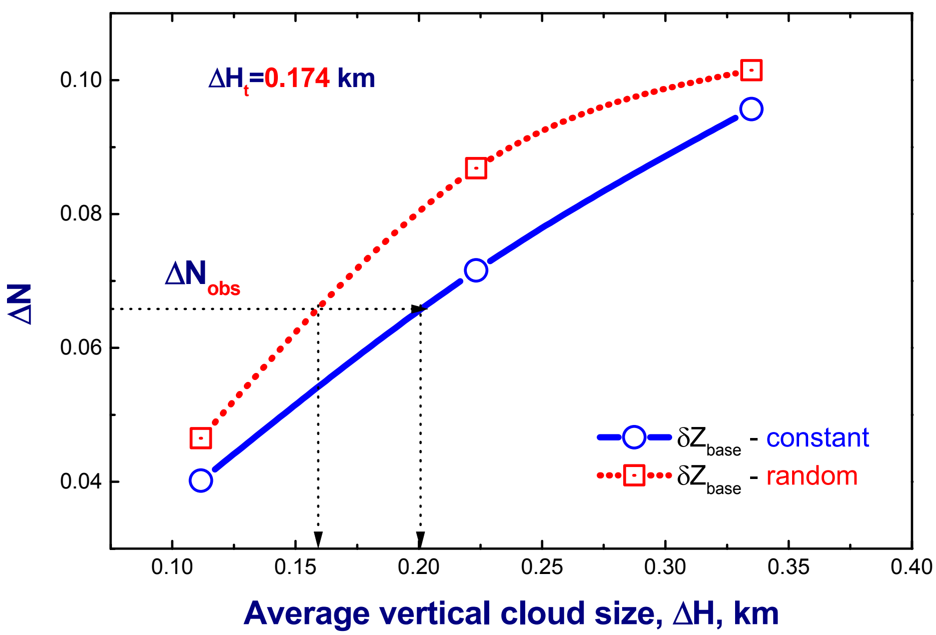

Figure 8. Difference ΔN_{mod} as a function of the average geometrical thickness ΔH_{avr} for two MISR-data experiments. The values of model parameters $\Delta H_{avr,\ const}$ and $\Delta H_{avr,\ random}$ such that $\Delta N_{mod,\ const}$ and $\Delta N_{mod,\ random}$ are equal to ΔN_{obs} are shown.

Summary

To evaluate the performance of new multi-angle cumulus geometry retrieval, both MISR data and ground-based observations at ARM TWP site (August 9, 2000) were applied. First, we tested this retrieval technique with simulated MISR observations by using an LES model and a Monte Carlo method (model-data inverse problem). It was demonstrated that the average cloud vertical size can be obtained with reasonable accuracy (about 0.1 km). In addition, we verified this retrieval technique with real MISR observations and independent ground-based radar measurements. It was shown that, satellite-retrieved average vertical thickness of cumulus clouds closely match (maximum difference about 0.03 km) the corresponding ground-truth value observed from radar measurements. We found that the accuracy of the cloud retrieval increases when additional information about cloud base variability is incorporated into the retrieval process. This information can be obtained from ground-based measurements (e.g., radar data). Since the comparison of satellite-retrieved products with ground-truth ones were made for a single MISR overpass, further testing over larger possible MISR scenes is needed to better understand the limits and accuracy of this retrieval technique.

Acknowledgments

This work was supported by the Office of Biological and Environmental Research of the U.S. Department of Energy as part of the ARM Program and by NASA under contract number 121164 with NASA/Jet Propulsion Laboratory (JPL).

Corresponding Author

E. I. Kassianov, Evgueni.Kassianov@pnl.gov; (509) 372-6535

References

Benner, T. C., and J. A. Curry, 1998: Characteristics of small tropical cumulus clouds and their impact on the environmental. *J. Geophys. Res.*, **103**, 28,753-28,767.

Clothiaux, E. E., K. P. Moran, B. E. Martner, T. P. Ackerman, G. G. Mace, T. Uttal, J. H. Mather, K. B. Widener, M. A. Miller, and D. J. Rodriguez, 1999: The Atmospheric Radiation Measurement cloud radars: operational modes. *J. Atmos. Sci.,* **56**, 819-827.

Dong, X., T. P. Ackerman, and E. E. Clothiaux, 1998: Parameterizations of the microphysical and shortwave radiative properties of boundary layer stratus from ground-based measurements. *J. Geophys. Res.*, **103**, 31681-31693.

Fox, N. I., and A. J. Illingworth, 1997: The potential of a spaceborne cloud radar for the detection of stratocumulus clouds. *J. Appl. Meteorol.*, **36**, 676–687.

Kassianov, E. I., T. P. Ackerman, and R. T. Marchand, 2000: Multi-angle remote sensing of cumulus geometry. In *Proceedings of the Tenth Atmospheric Radiation Measurement (ARM) Science Team Meeting,* U.S. Department of Energy, Washington, D.C. Available URL: http://www.arm.gov/docs/documents/technical/conf_0003/kassianov(2)-ei.pdf

Minnis, P., P. W. Heck, D. Y. Young, C. W. Fairall, and J. B. Snider, 1992: Stratocumulus cloud properties derived from simultaneous satellite and island-based instrumentation during FIRE. *J. Appl. Meteorol.*, **31**, 317-339.

Soulen P. F., M. D. King, S.-C. Tsay, G. T. Arnold, and J. Y. Li, 2000: Airborne spectral measurements of surface-atmosphere anisotropy during the SCAR-A, Kuwait oil fire, and TARFOX experiments. *J. Geophys. Res.*, **105**, 10,203-10,218.